

Iron(II) and iron(III) complexes containing ethynyl thiophene fragments

Séverine Roué, Claude Lapinte *

Organométalliques et Catalyse: Chimie et Electrochimie Moléculaire, UMR CNRS 6509, Université de Rennes 1, Institut de chimie de Rennes, Campus de Beaulieu, Bat 10C, F35042 Rennes, France

Received 23 July 2004; accepted 6 October 2004

Available online 13 November 2004

Abstract

The synthesis of the new complexes $\text{Cp}^*(\text{dppe})\text{Fe}-\text{C}\equiv\text{C}-2,5\text{-C}_4\text{H}_2\text{SR}$ ($\text{Cp}^* = 1,2,3,4,5\text{-pentamethylcyclopentadienyl}$; $\text{dppe} = 1,2\text{-bis(diphenylphosphino)ethane}$; **2a**, $\text{R} = \text{C}\equiv\text{CH}$; **2b**, $\text{R} = \text{C}\equiv\text{C}-\text{Si}(\text{CH}_3)_3$; **2c**, $\text{R} = \text{C}\equiv\text{C}-\text{Si}(\text{CH}(\text{CH}_3)_2)_3$; **3a**, $\text{R} = \text{C}\equiv\text{C}-2,5\text{-C}_4\text{H}_2\text{S}-\text{C}\equiv\text{CH}$; **3c**, $\text{R} = \text{C}\equiv\text{C}-2,5\text{-C}_4\text{H}_2\text{S}-\text{C}\equiv\text{C}-\text{Si}(\text{CH}(\text{CH}_3)_2)_3$) is described. The ^{13}C NMR and FTIR spectroscopic data indicate that the π -back donation from the metal to the carbon rich ligand increases with the size of the organic π -electron systems. The new complexes were also analyzed by CV and the chemical oxidation of **2a** and **3c** was carried out using 1 equiv of $[\text{Cp}_2\text{Fe}][\text{PF}_6]$. The corresponding complexes **2a** $[\text{PF}_6]$ and **3c** $[\text{PF}_6]$ are thermally stable, but **2a** $[\text{PF}_6]$ was too reactive to be isolated as a pure compound. The spectroscopic data revealed that the coordination of large organic π -electron systems to the iron nucleus produces only a weak increase of the carbon character of the SOMO for these new organoiron(III) derivatives.

© 2004 Elsevier B.V. All rights reserved.

Keywords: Organoiron; Iron(II); Iron(III); Acetylides; Ethynylthiophene; Redox-active

1. Introduction

The development of organometallic molecular assemblies incorporating metal atoms in organic π -networks has aroused a great deal of interest, owing to the fascinating properties that these combinations exhibit [1–9]. Over the past decade, we have been engaged in the study of redox-active organoiron compounds featuring several electroactive $\text{Cp}^*(\text{dppe})\text{Fe}$ units linked together, either directly through polyynyl bridges or via a central arene by means of ethynyl linkers [10–20]. Depending on their structures and on the oxidation states of the iron centers, these molecules exhibit electronic properties potentially useful for the realization of various molecular-scale devices [1,2]. More recently, we have shown

that molecules in which an electron-rich and redox-active $\text{Cp}^*(\text{dppe})\text{Fe}$ unit is connected to a different metal center through organic π -networks also possess fascinating properties [21–24]. At the same time, we also found that replacement of a phenyl unit by a thiophene ring in the carbon-rich bridges which link the organoiron units significantly improved the electronic and magnetic interactions between the metal centers [16,25].

The synthesis of new molecular architectures incorporating organometallic centers connected by extended π -networks requires the development of new synthons. We recently described the preparation and basic properties of the pivotal building block $\text{Cp}^*(\text{dppe})\text{FeC}\equiv\text{C}-1,4\text{-C}_6\text{H}_4-\text{C}\equiv\text{CH}$ [26], and now our interest is focused on the access to parent compounds containing thiophene rings as depicted on Chart 1.

In the electron-rich $\text{Cp}^*(\text{dppe})\text{Fe}$ series, isolation and purification of the mononuclear complexes are sometimes difficult and therefore the development of selective

* Corresponding author. Tel.: 33 2 23 23 59 63; fax: 33 2 23 23 59 63.

E-mail address: claude.lapinte@univ-rennes1.fr (C. Lapinte).

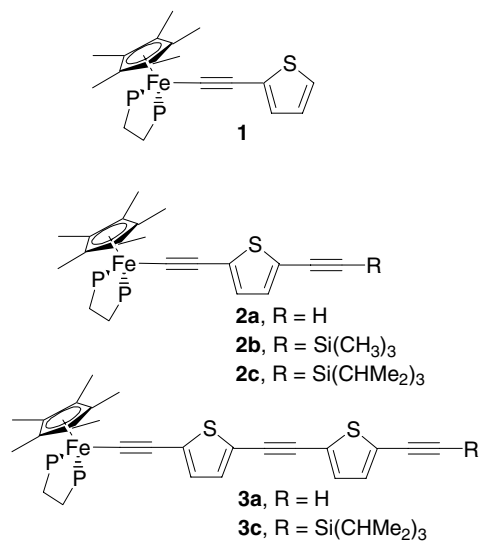
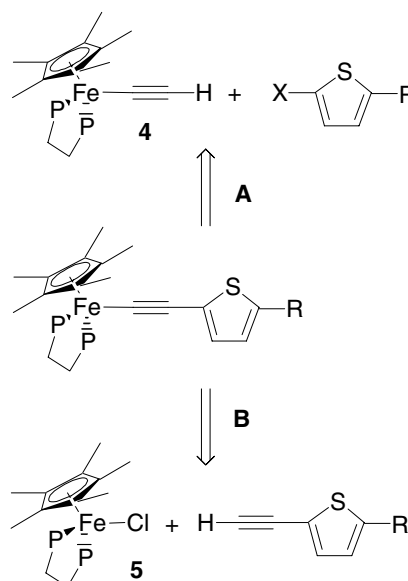


Chart 1.

reactions is highly desirable. We have previously found a “metalla-Sonogashira” coupling reaction [17,18], which allowed us to specifically graft various substituted bromo-aromatics onto the Cp*(dppe)FeCCH complex [27,28]. Using such an approach, Bruce et al. [29,30] also succeeded in functionalizing various terminal diynyl Mo(II) or W(II) complexes. Thus, starting from the organometallic terminal alkynyl complex Cp*(dppe)-FeC≡CH (**4**), various organoiron(II) derivatives containing halogeno-substituted thiophene fragments could be prepared (route A, Scheme 1). An alternative route to the target molecules can also consist in the initial preparation of the organic fragment and then, to its complexation to the Cp(dppe)FeCl (**5**) complex in a last step (route B, Scheme 1). We now report on (i) the



Scheme 1.

preparation of the organic precursors **8–10**, (ii) the syntheses of the complexes **2a–c** and **3a–c**, (iii) their characterization and redox properties, (iv) the preparation of the parent iron(III) derivatives **2a**[PF₆] and **3c**[PF₆] and (v) the optical properties of these new iron compounds.

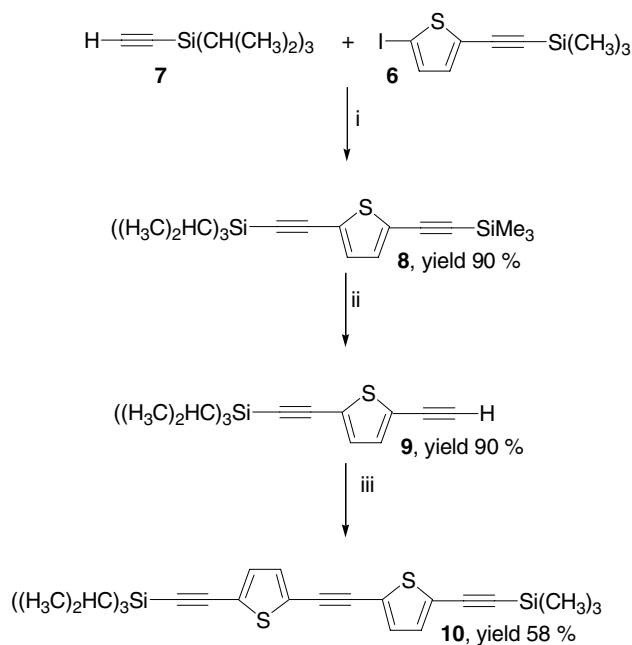
2. Results

2.1. Preparation of the organic precursors **8–10**

The non-symmetrical bis(ethynyl)thiophene **8** was prepared by a Sonogashira coupling reaction following procedures reported in the literature. The palladium–copper catalysed reaction between the known 2-iodo-(5-trimethylsilylethynyl)thiophene **6**, and the (tris(isopropyl)silyl)acetylene **7**, gave **8** in 90% yield after chromatography on a silica column (Scheme 2). Treatment of **8** with potassium carbonate in methanol at 20 °C allows the facile and selective cleavage of the trimethylsilyl terminal group and affords **9** in 90% yield after purification. Similarly, the palladium–copper catalyzed coupling between **6** and **9** provides **10** in 58% yield after chromatography.

2.2. Synthesis of the iron complex **2a** via **2b** and **2c**

The complexes Cp*(dppe)Fe–C≡C–C₄H₂S–C≡CSiR₃ (**2b**, **2c**) were prepared by two different routes (Scheme 3). The palladium coupling reaction in the coordination sphere of iron was extended to the



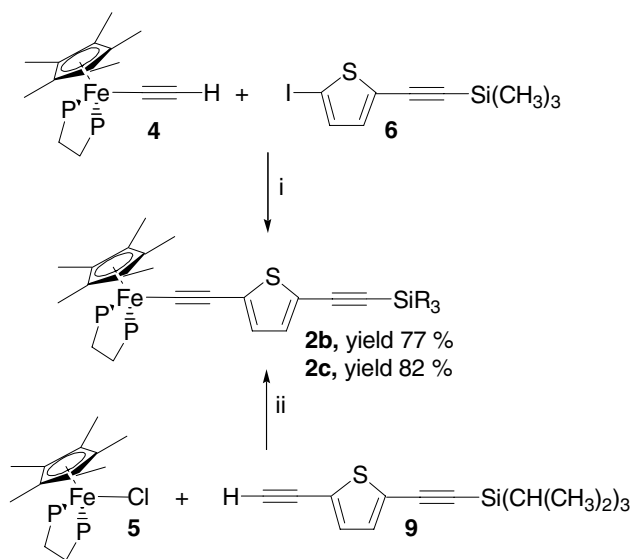
Scheme 2. Key reagents: (i) (Ph₃P)₂PdCl₂, CuI, ((CH₃)₂CH)₂NH, THF; (ii) MeOH, K₂CO₃; (iii) **6**, THF, (Ph₃P)₂PdCl₂, CuI, ((CH₃)₂CH)₂NH.

preparation of iron complexes containing thiophene rings. The terminal iron alkynyl complex **4** reacts with **6** in the presence of the Pd/Cu catalyst leading to isolation of **2b** in 77% yield. Alternatively, the chloro iron derivative Cp*(dppe)FeCl **5** reacts with the terminal organic alkyne **9** to produce **2c** via the corresponding vinylidene intermediate which is in situ deprotonated by addition of 1 equiv. of KOBu^t before removal of the solvent. From a synthetic standpoint, this route compares favourably with the Sonogashira coupling reaction in the coordination sphere giving **2c** as a pure orange powder in 82% yield. It can be noted in contrast, that the “metalla-Sonogashira” route was preferred to access to similar compounds containing benzene cycles instead of thiophene rings [18].

Carried out at 20 °C, the cleavage of the SiR₃ group provides **2a** in 85% yield either from **2b** or **2c**. However different conditions must be used in these two cases. The complex **2b** was reacted in a MeOH/THF (v/v: 50/50) mixture with potassium carbonate whereas, **2c** required a treatment with tetrabutylammonium fluoride in THF. The complexes **2a–c** were characterized by the usual techniques (see Section 4).

2.3. Synthesis of the iron complex **3a** via **3c**

The complexes containing two thiophene rings connected by an ethynyl fragment were prepared following a similar procedure (Scheme 4). The complex **2a** reacts with **6** in the presence of the Pd/Cu catalyst. The reaction reaches completion after 48 h at 50 °C and provides a pink powder which contains **3b** and the complex Cp*(dppe)Fe–C≡C–2,5-C₄H₂S–C≡C–C≡C–2,5-C₄H₂S–C≡C–Fe(dppe)Cp* **11**. This side prod-



Scheme 3. Key reagents: (i) (Ph₃P)₂PdCl₂, CuI, ((CH₃)₂CH)₂NH; (ii) NaBPh₄, MeOH, KOBu^t.

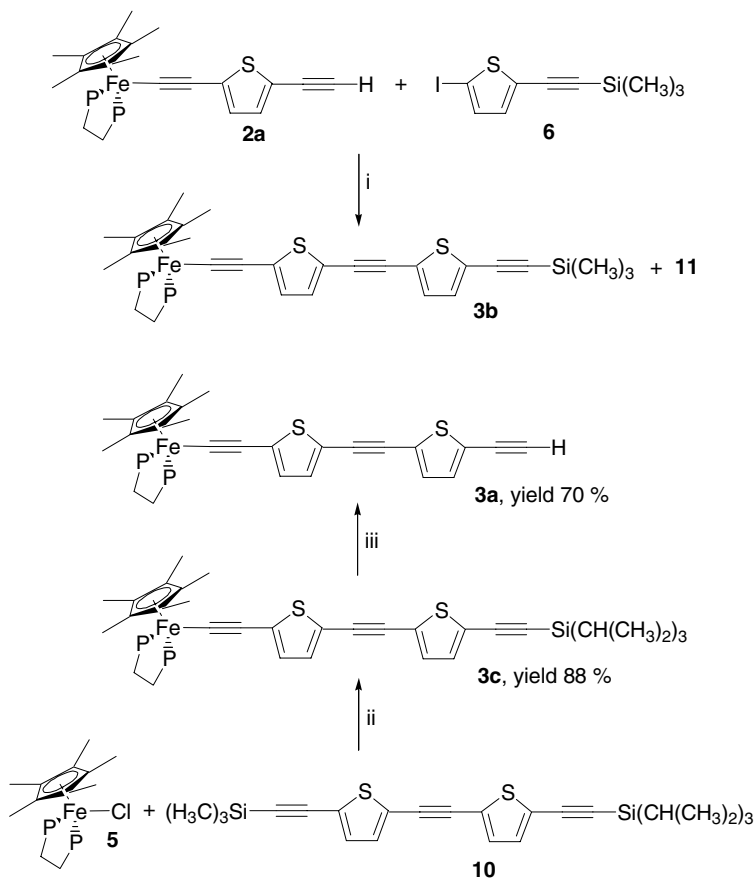
uct which results from the homocoupling between two molecules of **2a** was identified by comparison to an authentic sample independently prepared [31]. The separation of **3b** and **11** present in ca. 20% in the mixture could not be achieved.

The alternative route B (Scheme 1) was more successful. The complex **3a** was prepared following a one-pot procedure involving two successive reactions. The reactor was charged with the iron halide **5**, sodium tetraphenylborate, potassium carbonate, the organic reagent **10** dissolved in THF, and methanol. In these conditions, the terminal alkyne H–C≡C–2,5-C₄H₂S–C≡C–2,5-C₄H₂S–C≡C–Si(CH₃)₂)₃ was in situ generated by reaction of **10** with K₂CO₃.

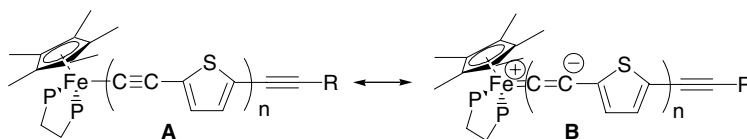
Then, the terminal organic alkyne reacts with the iron complex **5** to give a vinylidene intermediate and the dark green color of the solution progressively turns red. Addition of 1 equiv. of KOBu^t promotes the deprotonation of the vinylidene and gives the target compound **3c**. The air sensitive complex **3c** was isolated as a dark red powder in 88% yield. Treatment of the complex **3c** with tetrabutylammonium fluoride in THF at 20 °C provided **3a** in 70% yield. The complexes **3a** and **3c** were characterized by the usual techniques (see Section 4).

For the series of complexes **1–3**, the analysis of the ¹³C NMR chemical shifts of the C_α carbon atoms shows that these resonances are very sensitive to the extension of the alkynyl ligands. As the number of carbon atoms in the π-system increases, the C_α signals are shifted downfield from (δ, ppm) 146.3 for **1** to 152.9–153.2 for **2a–c** and to 155.9–156.2 for **3a–c**. This observation is in accordance with the increase of the electron-withdrawing effect of the organic carbon-rich ligand with the extension of its π-system [32]. In organometallic complexes, as the length of a carbon-rich ligand increases, its electron-withdrawing effect on the metal increases and induces a stronger π-back-bonding response from the metal center, the intensity of which being also related to how electron rich the metal is. Related effects have been observed for the complexes Cp*(dppe)Fe–C_x–Fe(dppe)Cp* with increasing *x* [33]. As a consequence, the cumulenic-type valence bond formulation **B** (Scheme 5) should contribute to the description of the electronic structure of the complexes, and as *n* increases, the weight of the structure **B** increases. As already pointed out, this effect concerns mainly the carbon atoms close to the metal centers and apparently does not propagate along the π-system [33].

The energy of the ν(C≡C) stretching modes corresponding to the CC triple bond adjacent to iron slightly decreases when the size of the carbon rich ligand increases (Table 1). The frequencies for this C≡C bond stretch (CH₂Cl₂, cm⁻¹) decrease by 10 cm⁻¹ and 15 cm⁻¹ from **1** to **2c** and from **1** to **3c**, respectively. Such behavior suggests a diminution of the bond order of the C_α≡C_β carbon–carbon triple bond as the π-electron



Scheme 4. Key reagents: (i) $(\text{Ph}_3\text{P})_2\text{PdCl}_2$, CuI, $((\text{CH}_3)_2\text{CH})_2\text{NH}$; (ii) NaBPh₄, MeOH, THF, K₂CO₃, KOBu^t; (iii) THF, TBAF.



Scheme 5.

system is extended. This is also in full agreement with a contribution of the canonical form **B** (Scheme 5) in the description of the electronic structures.

2.4. Cyclic voltammetry **2a–c**, **3a** and **3c**

The cyclic voltammograms (CV) of the complexes display a reversible one-electron wave (Table 2) in the range 0.5/–0.5 V vs the standard calomel electrode (SCE). This reversible process corresponds to the well-known metal-centered Fe(II)/Fe(III) oxidation and it indicates that the Fe(III) analogues are stable on the Pt electrode. It appears that the nature of the terminal group (H, Me₃Si or ^tPr₃Si) has almost no effect on the redox potentials. Comparison of the redox potentials of the complexes **2a–c** and **3a–c** with those of **1**, shows that the progressive extension of the π -system of the ligand increases the oxidation potentials indicating that the

energy level of the HOMO increases with the extent of the conjugation of the σ -alkynyl ligand.

It can also be observed that the substitution of the terminal alkyne of complex **4** by a ethynylthiophene group decreases the Fe^{II}/Fe^{III} redox potential by 0.13 V indicating that the presence of the thiophene ring on the alkyne ligand contributes to increase the energy level of the HOMO. In this respect, it can be observed that the effect of a benzene ring at the same position is less pronounced by 0.05 V [18]. However, the addition of alkyne or thiophene-alkynyl fragments on **1** has the opposite effect, since the redox potentials of **2a–c** and **3a–c** are less negative than that of **1**.

2.5. Oxidation of **2a** and **3c**

As suggested by the CVs the oxidized forms of **2a–b** and **3a–c** should be thermally stable. Accordingly, we

Table 1
FTIR data

Compd.	$\nu_{\text{C}\equiv\text{C}}$ Nujol	$\nu_{\text{C}\equiv\text{C}}$ CH ₂ Cl ₂	$\nu_{\text{C}\equiv\text{C}-\text{H}}$ Nujol	$\nu_{\text{C}\equiv\text{C}-\text{H}}$ CH ₂ Cl ₂	Ref.
1	2044	2040			[25]
2a	2090 2030 ^b	2087 2028 ^b	3289	3300	This work
2b	2132 2034 ^b	2131 2029 ^b			This work
2c	2136 2029 ^b	2130 2028 ^b			This work
3a	2180 2100 2025 ^b	2178 2101 2025 ^b	3300	3300	This work
3c	2180 2140 2030 ^b	2179 2139 2025 ^b			This work
4	1910 ^b				[10]
1[PF₆]	1977 ^b 1965 ^a	1963 ^b			[25]
2a[PF₆]	1942	1939	3277	3298	This work
3c[PF₆]	2182 2139 1947 ^b	2183 2141 1947 ^b			This work

^a Shoulder.^b C≡C triple bond identified as adjacent to Fe.Table 2
Electrochemical Data

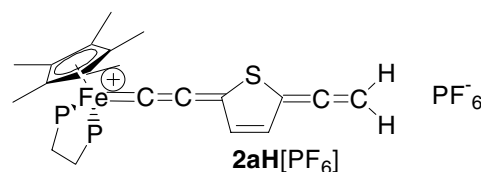
Compound	E^0	ΔE_p	(i_{pa}/i_{pc})	Reference
1	-0.14	0.09	1	[25]
2a	-0.08	0.70	1	This work
2b	-0.08	0.80		This work
2c	-0.09	0.07	1	This work
3a	-0.07	0.07	1	This work
3c	-0.07	0.07	1	This work
4	-0.01	0.10	0.8	[10]
12^a	-0.09	0.07	1	[13,18]

Potentials in CH₂Cl₂ (0.1 M [nBu₄N][PF₆], 20 °C, Pt electrode, sweep rate 0.100 V s⁻¹) are given in V vs SCE; the ferrocene–ferrocenium couple (0.460 V vs SCE) was used as an internal calibrant for the potential measurements.

^a Cp*(dppe)FeC≡C–C₆H₅.

have reacted **2a** and **3c** with [(η-C₅H₅)₂Fe][PF₆] to generate the corresponding paramagnetic salts **2a**[PF₆] and **3c**[PF₆]. The complex **3c**[PF₆] was isolated in a pure form as a thermally stable, dark red powder in 90% yield. In contrast, complex **2a**[PF₆] was always obtained as a mixture with a diamagnetic complex **2aH**[PF₆] in the 3:2 ratio. The separation of **2a**[PF₆] and **2aH**[PF₆] could not be achieved. In addition, the NMR characterization of **2aH**[PF₆] in the presence of the paramagnetic compound **2a**[PF₆] was unsuccessful. In accordance with the MS data, it appears that **2aH**[PF₆] differs from **2a**[PF₆] by only one hydrogen atom. As the IR spectrum of **2aH**[PF₆] does not show an absorption characteristic

of vinylidene derivatives in the range 1600–1650 cm⁻¹, it was assumed that the hydrogen atom was bound to the carbon in the terminal position providing a complex with a cumulene-type structure (Scheme 6). Mössbauer

Scheme 6. Proposed structure for complex **2aH**[PF₆].

spectroscopy supports this assumption. Indeed, the Mössbauer spectrum recorded at 80 K for the mixture of **2a**[PF₆] and **2aH**[PF₆] displays two doublets in the 3:2 ratio. The parameters of these doublets are quite different (**2a**[PF₆]: IS = 0.238 mm/s vs Fe, QS = 0.960 mm/s; **2aH**[PF₆]: IS = 0.100 mm/s vs Fe, QS = 1.237 mm/s), and consistent with the proposed structures for the two compounds. The parameters of **2aH**[PF₆] are typical of Fe^{II} complexes with an iron-carbon double bond, as previously shown for many related compounds of the Cp*(dppe)Fe family. The Mössbauer parameters of the complex **2a**[PF₆] are typical for 17-electron low spin Fe^{III} derivatives and very close to those obtained for compound **1**[PF₆] (IS = 0.227 mm/s vs Fe, QS = 0.974 mm/s).

A Mössbauer spectrum was also obtained at 80 K for the complex **3c**[PF₆]. It shows a unique doublet (IS = 0.236 mm/s vs Fe, QS = 0.918 mm/s) indicating that the oxidation of **3c** was quantitative. As expected, these data are quite close to those obtained for **1**[PF₆] and **2a**[PF₆]. For these three complexes, the IS values are similar in the accuracy of the measurements. One can note a small but significant and continuous decreases of the QS values from **1**[PF₆] to **2**[PF₆] and **3c**[PF₆]. This observation could be related to the variation of the metallic character of the HOMO as the size of the electron π -system increases.

The ESR spectra were run at 77 K in rigid glass (CH₂Cl₂/C₂H₄Cl₂) for samples of **2a**[PF₆] and **3c**[PF₆].

They display three features corresponding to the three components of the g-tensor, as expected for a d⁵ low-spin Fe^{III} radical in a pseudo-octahedral geometry (Table 3). In the case of the complex **3c**[PF₆] the two low field features are split into 1:2:1 triplet by hyperfine coupling with the two equivalent ³¹P nuclei. A similar observation was previously reported for the related compound **1**[PF₆]. The ESR parameters given Table 3 compare well with those of other mononuclear complexes of the same series. Comparison of the data shows that the g_{iso} and Δg tensors are significantly smaller for the complexes containing thiophene rings (**1**[PF₆], **2a**[PF₆], **3c**[PF₆]) than for those bearing a hydrogen atom (**4**[PF₆]) or a phenyl ring (**12**[PF₆]) on the alkynyl ligand. These experimental data suggest that one of the effects of the thiophene rings should be to decrease the metal character of the LUMO and the HOMO-LUMO energy gap.

2.6. Optical spectroscopies

Solutions of the complexes **1–3** range from orange to red as the length of the metal-alkynyl ligand increases. As shown in Table 4, the Fe^{II} complexes, **1–3**, present two high energy absorption bands which can be attributed to intraligand (IL) $\pi \rightarrow \pi^*$ transitions of the Cp* and dppe ligands. These bands have already been observed for other complexes containing the Cp*(dppe)Fe organometallic building block. However, in the cases of

Table 3
ESR parameters for compounds **1**[PF₆], **2a**[PF₆] and **3c**[PF₆]

Cmpd	g_1 (A _P)	g_2 (A _P)	g_3	g_{iso}	Δg
1 [PF ₆] ^a	1.986 (16 G)	2.036 (14 G)	2.366	2.129	0.380
2a [PF ₆]	1.985	2.035	2.385	2.135	0.400
3c [PF ₆]	1.988 (14 G)	2.036 (13 G)	2.363	2.129	0.375
4 [PF ₆] ^b	1.977	2.034	2.457	2.156	0.480
12 [PF ₆] ^c	1.975	2.033	2.464	2.157	0.489

^a From [25].

^b From [10].

^c [Cp*(dppe)FeC≡C–C₆H₅][PF₆] (see [13]).

Table 4
UV-vis data and tentative assignment of the electronic transitions

Compound	$\pi \rightarrow \pi^*$ λ nm ($10^{-3} \epsilon$ M ⁻¹ dm ³ cm ⁻¹)	MLCT λ nm ($10^{-3} \epsilon$ M ⁻¹ dm ³ cm ⁻¹)	LMCT λ nm ($10^{-3} \epsilon$ M ⁻¹ dm ³ cm ⁻¹)	Reference
1	233 (31.0), 273 (13.7)	362 (6.9)		[25]
2a	242 (31.3), 300 (13.4)	432 (12.2)		This work
2b	248 (20.8), 300 (11.9)	439 (10.3)		This work
2c	274 (29.4), 250 (26.7)	440 (17.3)		This work
3a	230 (54.0), 350 (22.4)	490 (21.9)		This work
3c	230 (36.4), 348 (25.5)	491 (19.2)		This work
1 [PF ₆]	273 (33.7), 402 (5.0)	434 (4.4)	736 (6.6)	[25]
3c [PF ₆]	230 (48.9), 262 (35.6), 388 (33.4)	502 (12.6)	584 (5.0), 884 (5.8)	This work

Table 5
NIR absorption data of **1**[PF₆], **2a**[PF₆] and **3c**[PF₆]

Cmpd	Band	ϵ (M ⁻¹ cm ⁻¹)	ν (cm ⁻¹)	$\Delta\nu_{\frac{1}{2}}$ (cm ⁻¹)	$\nu_A - \nu_B$ (cm ⁻¹)
1 [PF ₆]	A	106	5680	2100	1945
	B	10	7625	1620	
2a [PF ₆]	A	125	5560	2400	1955
	B	20	7515	1620	
3c [PF ₆]	A	210	6150	2260	1960
	B	20	8090	1800	

the complexes **1–3** their intensities are larger and depend on the number of thienyl fragments present in the compounds suggesting that $\pi \rightarrow \pi^*$ transitions of the C₄H₂S ring should overlay with those of the ancillary ligands.

With reference to the electronic absorption studies of monometallic complexes with similar structures like Cp*(dppe)Fe—C≡C—C₆H₅, [18], which show low energy absorptions in the range 340–450 nm, the low energy absorptions observed in the spectra of the complexes **1–3** are attributed to $d\pi\text{Fe} \rightarrow \pi^*(\text{C}\equiv\text{C})$ metal-to-ligand charge transfer transitions (MLCT). As the number of alkynyl and thiophene fragments increases, the MLCT transition is red shifted by ca. 80 nm from **1** to **2a–c** and by ca. 50 nm from **2a–c** to **3a–c**, while the intensities of the bands is increased.

The spectrum of Fe^{III} cation **3c**[PF₆] displays, besides the supposed MLCT band at 502 nm which is less intense and slightly red-shifted with respect to **3c**, two bands at lower energies. These bands are characteristic of Fe^{III} complexes and may be attributed to ligand-to-metal charge transfer (LMCT) transitions from low-lying ligand-based molecular orbitals (MO) to the half-filled HOMO, which is mainly metallic in character. A similar transition was also observed for the related complexes [15], but, in general, only one LMCT band was observed at a higher energy. As a result, the extension of the π -system of the carbon rich ligand increases the number of LMCT transitions and produces a red shift for the lower energy band.

The spectra of Fe^{II} complexes **1–3** do not present any absorption bands in the NIR range. In contrast, the NIR spectra of the corresponding Fe^{III} congeners contain absorption bands of weak intensities (Table 5). While the more intense bands are located at very similar energies for **1**[PF₆] and **2a**[PF₆], with an extinction coefficient close to 100 M⁻¹ dm⁻³ cm⁻¹, like all the Fe^{III} complexes of the Cp*(dppe)Fe series that we have previously characterized, the complex **3c**[PF₆] displays a more intense ($\epsilon = 210 \text{ M}^{-1} \text{ l}^{-1} \text{ cm}^{-1}$), red shifted absorption at ca. 6150 cm⁻¹ [14,34]. These bands correspond to forbidden ligand field transitions specific to the Cp*(dppe)Fe fragment. In addition, the NIR spectra of the three complexes **1**[PF₆], **2a**[PF₆] and **3c**[PF₆] show a second, very weak absorption band at ca. 2000 cm⁻¹ lower in energy, corresponding to the resolution of the

vibronic coupling with the $\nu(\text{Fe}-\text{C}\equiv\text{C})$ stretching modes of vibration (see Tables 1 and 2).

3. Conclusions

In this contribution, we have reported efficient synthetic access to new organoiron(II) containing thiophene acetylide fragments and have fully characterized these species. We have also prepared the relative organoiron(III) complexes and shown that these radicals are thermally stable. However, when the carbon-rich ligands are not substituted by a bulky terminal group, the species are very reactive and could not be isolated in pure form. Despite the presence of a ligand containing an extended π -electron system with up to fourteen sp or sp² hybridized carbon atoms bound to the 17-electron d⁵ iron center, these complexes can be regarded as metal centered radicals. The spectroscopic data revealed only a weak increase of the carbon character of the SOMO.

4. Experimental

4.1. General data

All manipulations were carried out under an argon atmosphere using Schlenk techniques or in a Jacomex 532 dry-box filled with nitrogen. Routine NMR spectra were recorded using a Bruker DPX 200 spectrometer. High field NMR spectra experiments were performed on a multinuclear Bruker WB 300 instrument. Chemical shifts are given in parts per million relative to tetramethylsilane (TMS) for ¹H and ¹³C NMR spectra, and H₃PO₄ for ³¹P NMR spectra. X-Band ESR spectra were recorded on a Bruker ESP-300E spectrometer. An Air Products LTD-3-110 liquid helium transfer system was attached for the low-temperature measurements. Cyclic voltammograms were recorded using a PAR 263 instrument with a SCE reference electrode and ferrocene as internal calibrant (0.460 V). The ⁵⁷Fe Mössbauer spectra were obtained by using a constant acceleration spectrometer previously described with a 50 mCi ⁵⁷Co source in a Rh matrix. The sample temperature was controlled by a Oxford MD306 cryostat and a Oxford ITC4 tem-

perature controller. Computer fitting of the Mössbauer data to Lorentzian line shapes was carried out with a previously described computer program [35,36]. The isomer shift values are reported with respect to iron foil at 298 K and are not corrected for the temperature-dependent second-order Doppler shift. The Mössbauer sample cell consists of a 2 cm diameter cylindrical plexiglass holder. Elemental analyses were performed at CRMPO, Rennes, France. LSI-MS analyses were performed at CRMPO on a high-resolution MS/MS ZabSpec TOF Micromass spectrometer (8 kV). The organic compound 2-iodo-5-(trimethylsilylethynyl)thiophene [37] and the organometallic complexes $\text{Cp}^*(\text{dppe})\text{FeCl}$ [38] and $\text{Cp}^*(\text{dppe})\text{FeC}\equiv\text{CH}$ [10] were prepared as previously described.

4.2. $((\text{CH}_3)_2\text{HC})_3\text{Si}-\text{C}\equiv\text{C}-2,5-\text{C}_4\text{H}_2\text{S}-\text{C}\equiv\text{C}-\text{Si}(\text{CH}_3)_3$ (**8**)

In a Schlenk tube, 0.520 g (1.70 mmol) 1-2,5- $(\text{C}_4\text{H}_2\text{S})-\text{C}\equiv\text{C}-\text{Si}(\text{CH}_3)_3$ **6**, 20 mL of THF, 0.026 g (0.136 mmol) of CuI, 0.048 g (0.068 mmol) of $(\text{Ph}_3\text{P})_2\text{PdCl}_2$, 5 mL of diisopropylamine and 0.43 mL (1.87 mmol) of (triisopropylsilyl)acetylene were successively added. The resulting solution was stirred for 16 h at 20 °C. Then 20 mL of water were added, and the mixture was extracted with CH_2Cl_2 . The organic phase was washed with a saturated solution of NaCl in water and dried over magnesium sulphate, filtered, and evaporated to provide a crude residue for purification. Column chromatography on silica gel eluted with hexane provided 0.551 g of **8** as an orange yellow liquid (1.53 mmol, 90%). Anal. Calc. for $\text{C}_{20}\text{H}_{32}\text{SSi}_2$: C, 66.60; H 8.94. Found: C, 66.48; H, 8.67. ^1H NMR (CDCl_3 , 200 MHz, 25 °C, δ , ppm) 7.07 (s, 2H, $\text{C}_4\text{H}_2\text{S}$), 1.16 (m, 21H, $\text{Si}(\text{CH}(\text{CH}_3)_2)_3$), 0.29 (s, 9H, $\text{Si}(\text{CH}_3)_3$). ^{13}C NMR (CDCl_3 , 50 MHz, 25 °C, δ , ppm) 132.6 (dd, $^1J_{\text{CH}} = 172$ Hz, $^2J_{\text{CH}} = 6$ Hz, C_4), 132.4 (dd, $^1J_{\text{CH}} = 172$ Hz, $^2J_{\text{CH}} = 6$ Hz, C_3), 125.4 (m, C_2), 124.7 (m, C_5), 100.1 (m, $\text{C}\equiv\text{C}-\text{Si}(\text{CH}_3)_3$), 99.2 (m, $\text{C}\equiv\text{C}-\text{Si}(\text{CH}(\text{CH}_3)_2)_3$), 97.4 (m, $\text{C}\equiv\text{C}-\text{Si}(\text{CH}(\text{CH}_3)_2)_3$), 97.2 (m, $\text{C}\equiv\text{C}-\text{Si}(\text{CH}_3)_3$), 19.1 (q, $^1J_{\text{CH}} = 126$ Hz, $\text{Si}(\text{CH}(\text{CH}_3)_2)_3$), 11.7 (d, $^1J_{\text{CH}} = 119$ Hz, $\text{Si}(\text{CH}(\text{CH}_3)_2)_3$), 0.20 (q, $^1J_{\text{CH}} = 121$ Hz, $\text{Si}(\text{CH}_3)_3$). FTIR (Nujol, KBr, ν , cm^{-1}) 2146 (s, $\text{C}\equiv\text{C}$).

4.3. $((\text{CH}_3)_2\text{HC})_3\text{Si}-\text{C}\equiv\text{C}-2,5-\text{C}_4\text{H}_2\text{S}-\text{C}\equiv\text{CH}$ (**9**)

In a flask 1.39 g (3.82 mmol) of **8** were dissolved in 40 mL of methanol before 0.635 g (4.59 mmol) of K_2CO_3 was added. The resulting mixture was stirred for 2 h at 20 °C, and the solvent was removed under reduced pressure. The crude residue was washed with diethyl ether (50 mL). The organic solution was washed with distilled water (60 mL), dried over magnesium sulphate, filtered and evaporated to provide **9** as a pure orange yellow liq-

uid (0.977 g, 3.4 mmol, 90%). Anal. Calc. for $\text{C}_{17}\text{H}_{24}\text{SSi}$: C, 70.77; H 8.38. Found: C, 70.45; H, 8.23. NMR ^1H (CDCl_3 , 200 MHz, 25 °C, δ , ppm) 7.12 (d, 1H, $^3J_{\text{HH}} = 3.8$ Hz, $\text{C}_4\text{H}_2\text{S}$), 7.08 (d, 1H, $^3J_{\text{HH}} = 3.8$ Hz, $\text{C}_4\text{H}_2\text{S}$), 3.36 (s, 1H, $\text{C}\equiv\text{C}-\text{H}$), 1.16 (s, 21H, $\text{Si}(\text{CH}(\text{CH}_3)_2)_3$). NMR ^{13}C (CDCl_3 , 50 MHz, 25 °C, δ , ppm) 133.1 (ddd, $^1J_{\text{CH}} = 171.8$ Hz, $^2J_{\text{CH}} = 6$ Hz, $^4J_{\text{CH}} = 2$ Hz, C_4), 132.4 (dd, $^1J_{\text{CH}} = 172$ Hz, $^2J_{\text{CH}} = 6$ Hz, C_3), 125.7 (m, C_2), 123.4 (m, C_5), 98.9 (d, $^3J_{\text{CH}} = 3$ Hz, $\text{C}\equiv\text{C}-\text{Si}(\text{CH}(\text{CH}_3)_2)_3$), 97.4 (m, $\text{C}\equiv\text{C}-\text{Si}(\text{CH}(\text{CH}_3)_2)_3$), 82.3 (d, $^1J_{\text{CH}} = 255$ Hz, $\text{C}\equiv\text{C}-\text{H}$), 76.8 (m, $^2J_{\text{CH}} = 51$ Hz, $^3J_{\text{CH}} = 4$ Hz, $\text{C}\equiv\text{C}-\text{H}$), 19.1 (q, $^1J_{\text{CH}} = 126$ Hz, $\text{Si}(\text{CH}(\text{CH}_3)_2)_3$), 11.7 (d, $^1J_{\text{CH}} = 119$ Hz, $\text{Si}(\text{CH}(\text{CH}_3)_2)_3$). FTIR (Nujol, KBr, ν , cm^{-1}): = 3310 (s, C-H), 2144 (s, $\text{C}\equiv\text{C}-\text{Si}(\text{CH}(\text{CH}_3)_2)_3$), 2104 (s, $\text{C}\equiv\text{C}-\text{H}$).

4.4. $((\text{CH}_3)_2\text{HC})_3\text{Si}-\text{C}\equiv\text{C}-2,5-\text{C}_4\text{H}_2\text{S}-\text{C}\equiv\text{C}-2,5-\text{C}_4\text{H}_2\text{S}-\text{C}\equiv\text{C}-\text{Si}(\text{CH}_3)_3$ (**10**)

In a Schlenk tube 0.935 g (3.05 mmol) of **6**, 30 mL of THF, 0.046 g (0.24 mmol) of CuI, 0.086 g (0.122 mmol) of $(\text{PPh}_3)_2\text{PdCl}_2$, 5 mL of diisopropylamine, and 0.970 g (3.36 mmol) of **9** were successively added. The solution was stirred for 16 h at 20 °C, and 50 mL of distilled water were added. After extraction with dichloromethane and washing with water, the organic extract was dried over magnesium sulfate and evaporated to provide a crude residue which was separated by column chromatography on silica gel eluted with hexane. Evaporation of the solvent under reduced pressure provide a yellow liquid identified as **10** (0.820 g, 1.76 mmol, 58%). Anal. Calc. for $\text{C}_{26}\text{H}_{34}\text{S}_2\text{Si}_2$: C, 72.25; H 8.08. Found: C, 72.07; H, 8.03. ^1H NMR (CDCl_3 , 200 MHz, 25 °C, δ , ppm) 7.12 (s, 4H, $\text{C}_4\text{H}_2\text{S}$), 1.15 (s, 21H, $\text{Si}(\text{CH}(\text{CH}_3)_2)_3$), 0.28 (s, 9H, $\text{Si}(\text{CH}_3)_3$). ^{13}C NMR (CDCl_3 , 75 MHz, 25 °C, δ , ppm) 133.0 (dd, $^1J_{\text{CH}} = 173$ Hz, $^2J_{\text{CH}} = 6$ Hz, C_4), 132.8 (dd, $^1J_{\text{CH}} = 172$ Hz, $^2J_{\text{CH}} = 4.8$ Hz, C_3), 132.5 (dd, $^1J_{\text{CH}} = 173$ Hz, $^2J_{\text{CH}} = 6$ Hz, $\text{C}_{4,3'}$), 126.1, 125.6, 124.3, 123.9 (4m, $\text{C}_{2,2',5,5'}$), 101.1 (m, $\text{C}\equiv\text{C}-\text{Si}(\text{CH}_3)_3$), 99.1 (m, $\text{C}\equiv\text{C}-\text{Si}(\text{CH}(\text{CH}_3)_2)_3$), 98.0 (m, $\text{C}\equiv\text{C}-\text{Si}(\text{CH}(\text{CH}_3)_2)_3$), 97.3 (m, $\text{C}\equiv\text{C}-\text{Si}(\text{CH}_3)_3$), 87.2 (m, $\text{C}\equiv\text{C}$), 86.9 (m, $\text{C}\equiv\text{C}$), 19.1 (qm, $^1J_{\text{CH}} = 126$ Hz, $\text{Si}(\text{CH}(\text{CH}_3)_2)_3$), 11.7 (dm, $^1J_{\text{CH}} = 123$ Hz, $\text{Si}(\text{CH}(\text{CH}_3)_2)_3$), 0.2 (q, $^1J_{\text{CH}} = 126$ Hz, $\text{Si}(\text{CH}_3)_3$). FTIR (Nujol, KBr, ν , cm^{-1}) 2144 (s, $\text{C}\equiv\text{C}$).

4.5. $\text{Cp}^*(\text{dppe})\text{Fe}-\text{C}\equiv\text{C}-\text{C}_4\text{H}_2\text{S}-\text{C}\equiv\text{CH}$ (**2a**)

(A). In a Schlenk tube, 0.632 g of $[\text{Cp}^*(\text{dppe})\text{Fe}-\text{C}\equiv\text{C}-2,5-(\text{C}_4\text{H}_2\text{S})-\text{C}\equiv\text{C}-\text{Si}(\text{CH}_3)_3]$ (**2b**, 0.80 mmol) and 0.110 g of K_2CO_3 (0.80 mmol) were dissolved in 50 mL of a MeOH/THF mixture ($\nu/\nu = 1:1$). The reaction mixture was stirred at 20 °C for 12 h and the solvents were removed in vacuo. The solid residue was extracted with toluene (3×10 mL) and the solvent removed in

vacuum. The resulting orange powder was washed with pentane (3 × 5 mL) and dried under vacuum. The complex **2a** was obtained as pure and thermally stable orange microcrystals (0.570 g, 0.79 mmol, 99%).

(B). To a THF solution (5 mL) of **2c** (1.000 g, 1.14 mmol), 0.23 mL of 1M solution of TBAF (0.23 mmol) was added. The resulting mixture was stirred at 20 °C for 16 h before the solvent was removed under reduced pressure. The crude residue was extracted with toluene (3 × 10 mL) and filtered on a silica pad (5 cm). Removal of the solvent in vacuum, washing with pentane (3 × 5 mL) and drying under vacuum yielded 0.681 g of complex **2a** (0.95 mmol, 83%). Anal. Calc. for C₄₄H₄₂FeP₂S: C, 73.33; H 5.87. Found: C, 73.61; H, 5.86. ¹H NMR (C₆D₆, 200 MHz, 25 °C, δ, ppm) 7.91–7.03 (m, 20H, Ph), 7.07 (d, 1H, ³J_{HH} = 3.8 Hz, C₄H₂S/H₄), 6.44 (d, 1H, ³J_{HH} = 3.8 Hz, C₄H₂S/H₃), 2.9 (s, 1H, ≡CH), 2.51–1.76 (2m, 4H, CH₂dpppe), 1.46 (s, 15H, C₅(CH₃)₅). ¹³C NMR (C₆D₆, 75 MHz, 25 °C, δ, ppm) 152.9 (t, ²J_{CP} = 38 Hz, C_α), 139.5–127.4 (m, Ph), 134.7 (m, C₂), 133.5 (dd, ¹J_{CH} = 168 Hz, ²J_{CH} = 6 Hz, C₄), 124.1 (dd, ¹J_{CH} = 168 Hz, ²J_{CH} = 6 Hz, C₃), 115.0 (m, C₅), 111.9 (t, ³J_{CP} = 2 Hz, C_β), 88.4 (s, C₅(CH₃)₅), 79.2 (d, ¹J_{CH} = 252 Hz, C_β'), 79.0 (dd, ²J_{CH} = 50 Hz, ³J_{CH} = 4 Hz, C_α'), 30.9 (m, ¹J_{CP} = 23 Hz, CH₂dpppe), 10.3 (q, ¹J_{CH} = 126 Hz, C₅(CH₃)₅). NMR {¹H} ³¹P (C₆D₆, 81 MHz, 25 °C, δ, ppm) 100.7 (s, dppe). FTIR (KBr/Nujol, ν, cm⁻¹) 3289 (m, ≡C–H), 2090 (w, C≡C), 2030 (s, C≡C).

4.6. Cp*(dppe)Fe–C≡C–2,5-C₄H₂S–C≡CSi(CH₃)₃ (**2b**)

To a Schlenk tube containing 0.500 g of the complex Cp*(dppe)Fe–C≡CH (**4**, 0.82 mmol), 0.057 g of (PPh₃)₂PdCl₂ (0.08 mmol) and 0.032 mg of CuI (0.16 mmol) 40 mL of di-*iso*-propylamine were added. With stirring, 0.505 g of 2-iodo-(5-triméthylsilyléthynyl)thiophène was added to the mixture, which was warmed for 24 h at 70 °C. After removal of the solvent under reduce pressure, the crude residue was extracted with toluene (3 × 10 mL) filtered on a celite pad and evaporated to dryness. Repeated washings with cold pentane (3 × 5 mL, –40 °C) and drying in vacuum, yielded **2b** as a pure orange powder (0.501 g, 0.63 mmol, 77%). Anal. Calc. for C₄₇H₅₀FeP₂SSi: C, 71.20; H, 6.36. Found: C, 70.65; H, 6.29. MS (positive LSI, *m*-NBA, *m/z*), 792 ([Cp*(dppe)Fe–C≡C–2,5-C₄H₂S–C≡CSi(CH₃)₃]⁺, 66%), 589 ([Cp*(dppe)Fe]⁺, 100%). HRMS (positive LSI, *m*-NBA, *m/z*) calc.: 792.2227, found: 792.2225. ¹H NMR (C₆D₆, 200 MHz, 25 °C, δ, ppm) 7.90–7.01 (m, 20H, Ph), 7.13 (d, 1H, ³J_{HH} = 3.8 Hz, C₄H₂S/C₄), 6.42 (d, 1H, ³J_{HH} = 3.8 Hz, C₄H₂S/C₃), 2.50–1.74 (2m, 4H, CH₂dpppe), 1.45 (s, 15H, C₅(CH₃)₅), 0.20 (s, 9H, Si(CH₃)₃). NMR ¹³C (C₆D₆, 75 MHz, 25 °C, δ, ppm) 153.2 (t, ²J_{CP} = 41 Hz, C_α), 139.5–127.4 (m, Ph), 134.7

(m, C₂), 133.3 (dd, ¹J_{CH} = 167 Hz, ²J_{CH} = 6 Hz, C₄), 124.2 (dd, ¹J_{CH} = 168 Hz, ²J_{CH} = 5 Hz, C₃), 116.2 (dd, ²J_{CH} = 13 Hz, ³J_{CH} = 5 Hz, C₅), 112.0 (s, C_β), 100.6 (d, ³J_{CH} = 4 Hz, C_α'), 95.8 (m, C_β'), 88.4 (s, C₅(CH₃)₅), 30.9 (m, ¹J_{CP} = 23 Hz, CH₂dpppe), 10.3 (q, ¹J_{CH} = 126 Hz, C₅(CH₃)₅), 0.2 (q, ¹J_{CH} = 118 Hz, Si(CH₃)₃). {¹H} ³¹P NMR (C₆D₆, 81 MHz, 25 °C, δ, ppm) 100.6 (s, dppe). FTIR (KBr/Nujol, ν, cm⁻¹) 2132 (m, C≡C), 2034 (s, C≡C).

4.7. Cp*(dppe)Fe–C≡C–2,5-C₄H₂S–C≡C–Si(CH₃)₂)₃ (**2c**)

In a Schlenk tube, 1.000 g of the complex Cp*(dppe)FeCl (**5**, 1.60 mmol), 0.602 g of NaBPh₄ (1.76 mmol) and 40 mL of methanol were introduced before adding 0.507 g of ((CH₃)₂CH)₃Si–C≡C–(C₄H₂S)–C≡C–H in THF (1.76 mmol in 10 mL of THF). The mixture was stirred at 20 °C for 16 h and then 0.197 g of KO^tBu was added (1.76 mmol). After stirring one additional hour, the solvents were removed in vacuum. The solid residue was extracted with dichloromethane (3 × 20 mL), the solvent removed in vacuum, the residue washed with cold pentane (3 × 10 mL, –60 °C). After drying in vacuum, 1.148 g of an orange powder of the compound **2c** were obtained (1.31 mmol, 82%). MS (positive LSI, *m*-NBA, *m/z*), 876 ([Cp*(dppe)Fe–C≡C–2,5-C₄H₂S–C≡C–Si(CH(CH₃)₂)₃]⁺, 66%), 741 ([dppe)Fe–C≡C–2,5-C₄H₂S–C≡C–Si(CH(CH₃)₂)₃]⁺, 3%), 589 ([Cp*(dppe)Fe]⁺, 100%). HRMS (positive LSI, *m*-NBA, *m/z*) calc.: 876.3166, found: 876.3184. ¹H NMR (C₆D₆, 200 MHz, 25 °C, δ, ppm) 7.91–7.01 (m, 20H, Ph), 7.08 (d, 1H, ³J_{HH} = 3.8 Hz, C₄H₂S/H₄), 6.42 (d, 1H, ³J_{HH} = 3.8 Hz, C₄H₂S/H₃), 2.51–1.77 (2m, 4H, CH₂dpppe), 1.46 (s, 15H, C₅(CH₃)₅), 1.20 (m, 21H, Si(CH(CH₃)₂)₃). ¹³C NMR (50 MHz, C₆D₆, 25 °C, δ, ppm) 153.2 (t, ²J_{CP} = 38 Hz, C_α), 139.7–127.5 (m, Ph), 134.7 (m, C₂), 133.4 (dd, ¹J_{CH} = 167 Hz, ²J_{CH} = 6 Hz, C₄), 124.2 (dd, ¹J_{CH} = 168 Hz, ²J_{CH} = 6 Hz, C₃), 116.0 (m, C₅), 112.4 (s, C_β), 102.6 (d, ³J_{CH} = 4 Hz, C_α'), 92.2 (s, C_β'), 88.5 (s, C₅(CH₃)₅), 31.1 (m, ¹J_{CP} = 23 Hz, CH₂dpppe), 19.2 (q, ¹J_{CH} = 126 Hz, Si(CH(CH₃)₂)₃), 10.4 (q, ¹J_{CH} = 120 Hz, Si(CH(CH₃)₂)₃), 10.4 (q, ¹J_{CH} = 126 Hz, C₅(CH₃)₅). {¹H} ³¹P NMR (C₆D₆, 81 MHz, 25 °C, δ, ppm) 100.8 (s, dppe). FTIR (KBr/Nujol, ν, cm⁻¹) 2136 (m, C≡C), 2029 (s, C≡C).

4.8. Cp*(dppe)Fe–C≡C–2,5-C₄H₂S–C≡C–2',5'-C₄H₂S–C≡CH (**3a**)

In a Schlenk tube, a 0.600 g of the complex [Cp*(dppe)Fe–C≡C–2,5-(C₄H₂S)–C≡C–2',5'-(C₄H₂S)–C≡C–Si(CH(CH₃)₂)₃] (**3c**, 0.61 mmol) was dissolved in 40 mL of THF before adding 122 μL of a 1M solution of TBAF

in THF (0.12 mmol). The mixture was stirred at 20 °C for 16 h and the solvent was removed. The crude residue was extracted with toluene (3 × 10 mL) and filtered over a silica pad. Removal of the solvent under reduce pressure, washing with cold pentane (2 × 10 mL, –40 °C) and evaporation to dryness yielded 0.352 g of **3a** isolated as a red powder (0.43 mmol, 70%). Anal. Calc. For C₅₀H₄₄FeP₂S₂: C, 72.63; H, 5.36; S, 7.76. Found: C, 72.84; H, 5.28; S, 7.31. MS (positive LSI, *m*-NBA, *m/z*), 826 ([Cp*(dppe)Fe–C≡C–2,5-C₄H₂S–C≡C–2,5-C₄H₂S–C≡CH]⁺, 100%), 691 ([Cp*(dppe)Fe–C≡C–2,5-C₄H₂S–C≡C–2,5-C₄H₂S–C≡CH]⁺, 7%), 589 ([Cp*(dppe)Fe]⁺, 67%). HRMS (positive LSI, *m*-NBA, *m/z*) calc.: 826.1709, found: 826.1707. ¹H NMR (C₆D₆, 200 MHz, 25 °C, δ, ppm) 7.91–7.05 (m, 21H, Ph + C₄H₂S/H₄), 6.73 (d, 1H, ³J_{HH} = 3.8 Hz, C₄H₂S/H₃), 6.65 (d, 1H, ³J_{HH} = 3.8 Hz, C₄H₂S/H₄), 6.48 (d, 1H, ³J_{HH} = 3.8 Hz, C₄H₂S/H₃), 2.79 (s, 1H, ≡C–H), 2.49–1.75 (2m, 4H, CH₂) 1.46 (s, 15H, C₅(CH₃)₅). ¹³C NMR (C₆D₆, 75 MHz, 25 °C, δ, ppm) 155.9 (t, ²J_{CP} = 38 Hz, C_α), 139.6–127.7 (m, Ph), 135.6 (s, C₂), 133.6 (dd, ¹J_{CH} = 168 Hz, ²J_{CH} = 6 Hz, C₄), 133.3 (dd, ¹J_{CH} = 171 Hz, ²J_{CH} = 6 Hz, C₄'), 131.2 (dd, ¹J_{CH} = 172 Hz, ²J_{CH} = 6 Hz, C₃'), 126.4 (m, C₂'), 124.5 (dd, ¹J_{CH} = 168 Hz, ²J_{CH} = 6 Hz, C₃), 123.0 (dd, ²J_{CH} = 12 Hz, ³J_{CH} = 6 Hz, C₅'), 114.8 (dd, ²J_{CH} = 12 Hz, ³J_{CH} = 6 Hz, C₅), 112.6 (s, C_β), 90.3 (d, ³J_{CH} = 4 Hz, C_α'), 88.5 (s, C₅(CH₃)₅), 83.9 (d, ³J_{CH} = 4 Hz, C_β'), 82.5 (d, ¹J_{CH} = 255 Hz, C_β'), 76.9 (dd, ²J_{CH} = 51 Hz, ³J_{CH} = 4 Hz, C_α'), 31.2 (m, ¹J_{CP} = 23 Hz, CH₂_{dppe}), 10.3 (q, ¹J_{CH} = 126 Hz, C₅(CH₃)₅). {¹H} ³¹P NMR (C₆D₆, 81 MHz, 25 °C, δ, ppm) 100.6 (s, dppe). FTIR (KBr/Nujol, ν, cm^{–1}) 3300 (m, ≡C–H), 2180 (m, C≡C), 2100 (w, C≡C), 2025 (s, C≡C).

4.9. Cp*(dppe)Fe–C≡C–2,5-C₄H₂S–C≡C–2,5-C₄H₂S–C≡C–Si(CH(CH₃)₂)₃ (**3c**)

Cp*(dppe)FeCl (**5**, 1.000 g, 1.60 mmol), NaBPh₄ (0.602 g, 1.76 mmol) and K₂CO₃ were dissolved in methanol (40 mL). Then, a THF solution (10 mL) containing 0.747 g of (CH₃)₃Si–C≡C–2,5-(C₄H₂S)–C≡C–2',5'-(C₄H₂S)–C≡C–Si(CH(CH₃)₂)₃ (**10**, 1.76 mmol) were added. Immediately, the greenish mixture turned red. The mixture was stirred for 16 h at 20 °C, then 0.197 g of KO^tBu (1.76 mmol) were added and after stirring one additional hour, the solvent was removed in vacuum. The solid residue was extracted with toluene (3 × 10 mL), the solvent was removed under reduce pressure and the powder was washed with cold pentane (2 × 20 mL, –60 °C) before being dried under vacuum. The complex **3c** was isolated as a pure purple-red powder (1.390 g, 1.41 mmol, 88%). Anal. Calc. for C₅₉H₆₄FeP₂S₂Si: C, 72.05; H, 6.56. Found: C, 71.93; H, 6.58. MS (positive LSI, *m*-NBA, *m/z*), 982 ([Cp*(dppe)Fe–C≡C–2,5-C₄H₂S–C≡C–2,5-C₄H₂S–

C≡C–Si(CH(CH₃)₂)₃]⁺, 96%), 847 ([Cp*(dppe)Fe–C≡C–2,5-C₄H₂S–C≡C–2,5-C₄H₂S–C≡C–Si(CH(CH₃)₂)₃]⁺, 6%), 589 ([Cp*(dppe)Fe]⁺, 67%). HRMS (positive LSI, *m*-NBA, *m/z*) calc.: 982.3043, found: 982.3045. ¹H NMR (C₆D₆, 200 MHz, 25 °C, δ, ppm) 7.91–6.99 (m, 20H, Ph), 7.04 (d, 1H, ³J_{HH} = 3.8 Hz, C₄H₂S/H₄), 6.77 (d, 1H, ³J_{HH} = 3.8 Hz, C₄H₂S/H₃), 6.66 (d, 1H, ³J_{HH} = 3.8 Hz, C₄H₂S/H₄), 6.48 (d, 1H, ³J_{HH} = 3.8 Hz, C₄H₂S/H₃), 2.49–1.75 (2m, 4H, CH₂), 1.46 (s, 15H, C₅(CH₃)₅), 1.13 (m, 21H, Si(CH(CH₃)₂)₃). ¹³C NMR (C₆D₆, 50 MHz, 25 °C, δ, ppm) 156.2 (t, ²J_{CP} = 38 Hz, C_α), 139.6–127.6 (m, Ph), 135.6 (s, C₂), 133.6 (dd, ¹J_{CH} = 168 Hz, ²J_{CH} = 6 Hz, C₄), 133.1 (dd, ¹J_{CH} = 171 Hz, ²J_{CH} = 6 Hz, C₄'), 131.4 (dd, ¹J_{CH} = 172 Hz, ²J_{CH} = 6 Hz, C₃'), 126.1 (m, C₂'), 124.6 (dd, ¹J_{CH} = 168 Hz, ²J_{CH} = 6 Hz, C₃), 124.3 (dd, ²J_{CH} = 12 Hz, ³J_{CH} = 6 Hz, C₅'), 114.9 (dd, ²J_{CH} = 12 Hz, ³J_{CH} = 6 Hz, C₅), 112.6 (s, C_β), 100.3 (d, ³J_{CH} = 4 Hz, C_α'), 96.8 (s, C_β'), 90.3 (d, ³J_{CH} = 4 Hz, C_α'), 88.6 (s, C₅(CH₃)₅), 84.2 (d, ³J_{CH} = 4 Hz, C_β'), 31.1 (m, ¹J_{CP} = 23 Hz, CH₂_{dppe}), 19.0 (q, ¹J_{CH} = 126 Hz, Si(CH(CH₃)₂)₃), 11.8 (d, ¹J_{CH} = 119 Hz, Si(CH(CH₃)₂)₃), 10.5 (q, ¹J_{CH} = 126 Hz, C₅(CH₃)₅). {¹H} ³¹P NMR (81 MHz, C₆D₆, 25 °C, δ, ppm) 100.6 (s, dppe). FTIR (KBr/Nujol, ν, cm^{–1}) 2180 (w, C≡C), 2140 (m, C≡C), 2030 (s, C≡C).

Acknowledgement

We thank A. Mari (LCC, Toulouse) for Mössbauer measurements. We are indebted to ANRT and Laboratoires Standa (Caen) for financial support and a thesis grant to S.R.

References

- [1] F. Paul, C. Lapinte, *Coord. Chem. Rev.* 178–180 (1998) 427.
- [2] F. Paul, C. Lapinte, in: B. Wrackmeyer (Ed.), *Unusual Structures and Physical Properties in Organometallic Chemistry*, John Wiley & sons, London, 2002, p. 220.
- [3] R. Ziessel, M. Hissler, A. El-gayhoury, A. Harriman, *Coord. Chem. Rev.* 178–180 (1998) 1251.
- [4] I.R. Whittall, A.M. MacDonagh, M.G. Humphrey, M. Samoc, *Adv. Organomet. Chem.* 43 (1998) 349.
- [5] V.W.-W. Yam, K.K.-W. Lo, K.M.-C. Wong, *J. Organomet. Chem.* 578 (1999) 3.
- [6] P.F.H. Schwab, M.D. Levin, J. Michl, *Chem. Rev.* 99 (1999) 1863.
- [7] R.E. Martin, F. Diederich, *Angew. Chem., Int. Ed. Engl.* 38 (1999) 1351.
- [8] R. Ziessel, *Synthesis* (1999) 1839.
- [9] V.W.-W. Yam, *Acc. Chem. Res.* 35 (2002) 555.
- [10] N. LeNarvor, L. Toupet, C. Lapinte, *J. Am. Chem. Soc.* 117 (1995) 7129.
- [11] N. LeNarvor, C. Lapinte, *Organometallics* 14 (1995) 634.
- [12] T. Weyland, Ph.D. Thesis, Rennes I (Rennes), 1997.
- [13] T. Weyland, K. Costuas, A. Mari, J.-F. Halet, C. Lapinte, *Organometallics* 17 (1998) 5569.

- [14] T. Weyland, K. Costuas, L. Toupet, J.-F. Halet, C. Lapinte, *Organometallics* 19 (2000) 4228.
- [15] T. Weyland, I. Ledoux, S. Brasselet, J. Zyss, C. Lapinte, *Organometallics* 19 (2000) 5235.
- [16] S. Le Stang, F. Paul, C. Lapinte, *Organometallics* 19 (2000) 1035.
- [17] S. Le Stang, F. Paul, C. Lapinte, *Inorg. Chim. Acta* 291 (1999) 403.
- [18] R. Denis, L. Toupet, F. Paul, C. Lapinte, *Organometallics* 19 (2000) 4240.
- [19] K. Costuas, F. Paul, L. Toupet, J.-F. Halet, C. Lapinte, *Organometallics* 23 (2004) 2053.
- [20] F. Paul, K. Costuas, I. Ledoux, S. Deveau, J. Zyss, J.-F. Halet, C. Lapinte, *Organometallics* 21 (2002) 5229.
- [21] F. Coat, M.-A. Guillevic, L. Toupet, F. Paul, C. Lapinte, *Organometallics* 16 (1997) 5988.
- [22] F. Paul, W.E. Meyer, L. Toupet, H. Jiao, J.A. Gladysz, C. Lapinte, *J. Am. Chem. Soc.* 122 (2000) 9405.
- [23] H. Jiao, K. Costuas, J.A. Gladysz, J.-F. Halet, M. Guillemot, L. Toupet, F. Paul, C. Lapinte, *J. Am. Chem. Soc.* 125 (2003) 9511.
- [24] K.M.-C. Wong, S.C.-F. Lam, C.-C. Ko, N. Zhu, V.W.-W. Yam, S. Roué, C. Lapinte, S. Fathallah, K. Costuas, S. Kahlal, J.-F. Halet, *Inorg. Chem.* 42 (2003) 7086.
- [25] S. Roué, S. Le Stang, L. Toupet, C. Lapinte, *C. R. Chim.* 6 (2003) 353.
- [26] J. Courmarcel, G. Le Glang, L. Toupet, F. Paul, C. Lapinte, *J. Organomet. Chem.* 670 (2003) 108.
- [27] P. Siemsen, R.C. Livingstone, F. Diederich, *Angew. Chem. Int. Ed.* 39 (2000) 2633.
- [28] S. Takahashi, Y. Kuroyama, K. Sonogashira, N. Hagihara, *Synthesis* (1980) 627.
- [29] M.I. Bruce, M. Ke, P.J. Low, B.W. Skelton, A.H. White, *Organometallics* 17 (1998) 3539.
- [30] M.I. Bruce, M. Ke, P.J. Low, *J. Chem. Soc. Chem. Commun.* (1996) 2405.
- [31] S. Roué, Ph.D. Thesis, Rennes 1 (Rennes), 2002.
- [32] R. Eastmond, T.R. Johnson, D.R.M. Walton, *J. Organomet. Chem.* 50 (1973) 87.
- [33] F. Coat, F. Paul, C. Lapinte, L. Toupet, K. Costuas, J.-F. Halet, *J. Organomet. Chem.* 683 (2003) 368.
- [34] F. Paul, C. Lapinte, work in progress.
- [35] F. Varret, J.-P. Mariot, J.-R. Hamon, D. Astruc, *Hyperfine Interact.* 39 (1988) 67.
- [36] N.N. Greenwood, *Mössbauer Spectroscopy*, Chapman and Hall, London, 1971.
- [37] E. Viola, C. Losterzo, F. Trezzi, *Organometallics* 15 (1996) 4352.
- [38] C. Roger, P. Hamon, L. Toupet, H. Rabaâ, J.-Y. Saillard, J.-R. Hamon, C. Lapinte, *Organometallics* 10 (1991) 1045.